# A pulsed field gradient and NMR imaging investigations of the water retention mechanism by cellulose ethers in mortars

Laetitia Patural [a,*], Patrice Porion [b], Henri Van Damme [c], Alexandre Govin [a], Philippe Grosseau [a], Bertrand Ruot [d], Olivier Devès [d]

[a] École Nationale Supérieure des Mines de Saint-Étienne, Centre SPIN, LPMG UMR 5148, 158 cours Fauriel, F-42023 Saint-Étienne Cedex 2, France
[b] Centre de la Recherche sur la Matière Divisée, CNRS-Université d'Orléans, UMR 6619, 1b rue de la Férollerie, F-45071 Orléans Cedex 2, France
[c] Laboratoire de Physico-chimie des Polymères et Milieux Dispersés, ESPCI ParisTech, 10 rue Vauquelin, F-75231 Paris Cedex 05 and Université Paris Est - LCPC, 58 boulevard Lefebvre, 75732 Paris cedex 15, France
[d] Université Paris-Est, Centre Scientifique et Technique du Bâtiment, Département Enveloppe et Revêtements/Division Enduits, Mortiers et Colles, 84 avenue Jean Jaurès, F-77447 Marne-la-Vallée Cedex 2, France

## ARTICLE INFO

## ABSTRACT

The study presented in this paper is devoted to improve the knowledge on the influence of cellulose ethers (CE) on the freshly-mixed mortars water retention. Indeed, this crucial property is the most important imparted by these polysaccharides. One of the assumptions proposed to explain this phenomenon is that CE acts as diffusion barrier to the water. To test this hypothesis, the CE effect on the self-diffusion coefficient of water in solution and on the water mobility between two fresh cement pastes was studied by Nuclear Magnetic Resonance. CE does not significantly modify the water self-diffusion coefficient in CE solution or in admixed cement pastes. Moreover the interdiffusion imaging experiments demonstrated that the water diffusion at the paste/paste interface is not affected by the presence of cellulosic admixture.

© 2010 Elsevier Ltd. All rights reserved.

## 1. Introduction

Cellulose ethers (CE) are water-soluble polymers derived from cellulose, the most abundant polysaccharide in Nature. This polymer is built up from 1,4-anhydroglucose units linked through β-1,4 glycosidic bonds. It is insoluble in water because of the tight connection of the paired cellulose chains *via* hydrogen bridges. These bonds can be disrupted by partial or total etherification of the cellulose hydroxyl groups with various organic groups, then turning the material into water-soluble. Among these derivatives, **h**ydro-xy**p**ropyl **m**ethyl **c**ellulose, HPMC (Fig. 1a), **h**ydroxy**e**thyl **m**ethyl **c**ellulose, HEMC (Fig. 1b) and **h**ydroxy**e**thyl **c**ellulose, HEC (Fig. 1c) are extensively used in the formulation of various industrial products such as food, pharmaceuticals, construction products, etc., thanks to their non-toxic character and their interesting rheological and mechanical properties. In building materials, such as mortars, cellulose derived products are used as water-retention agents, thickeners, and film formers.

Water retention is the most important property imparted to CE when used in a cement based mortar. The water retention capacity of neat cementitious pastes submitted to a hydric stress (evaporation,

filtration under pressure, or suction by the substrate) is poor and organic admixtures are generally added when strong water retention is required [1]. Cellulose derivatives are the most suitable molecules used to improve this property. This specific behaviour of CE is particularly crucial when the mortar is applied in thin layers on highly absorbent substrates (that is, in conditions where water loss is occurring by evaporation and by suction). Cellulosic admixtures are added in order to retain the amount of water required for proper hydration and setting of the cement and to achieve sufficient mortar-substrate adhesion.

In spite of the success of CE in practical applications, little work has been devoted to the mechanism of their remarkable water retention capacity [2]. Pourchez et al. characterized some HPMC, HEMC and HEC in terms of water retention [3–5]. A significant influence of the polymer molecular parameters (i.e. molecular weight and substitu-tion degrees) was evidenced, but no clear water retention mechanism could be identified. One hypothesis was put forward concerning the water bound to cellulose ethers. Nevertheless, cryo-differential scanning calorimetry was used to quantify the bound water with the results that water bound to CE was not responsible for strong water retention capacities [3].

The concept of water retention itself covers different properties, depending on whether one is interested in limiting water evapora-tion, or limiting water loss to a porous substrate, or both. During evaporation, no admixture loss is occurring, due to the very low

* Corresponding author. Tel.: +33 4 77 49 97 77; fax: +33 4 77 49 96 94.
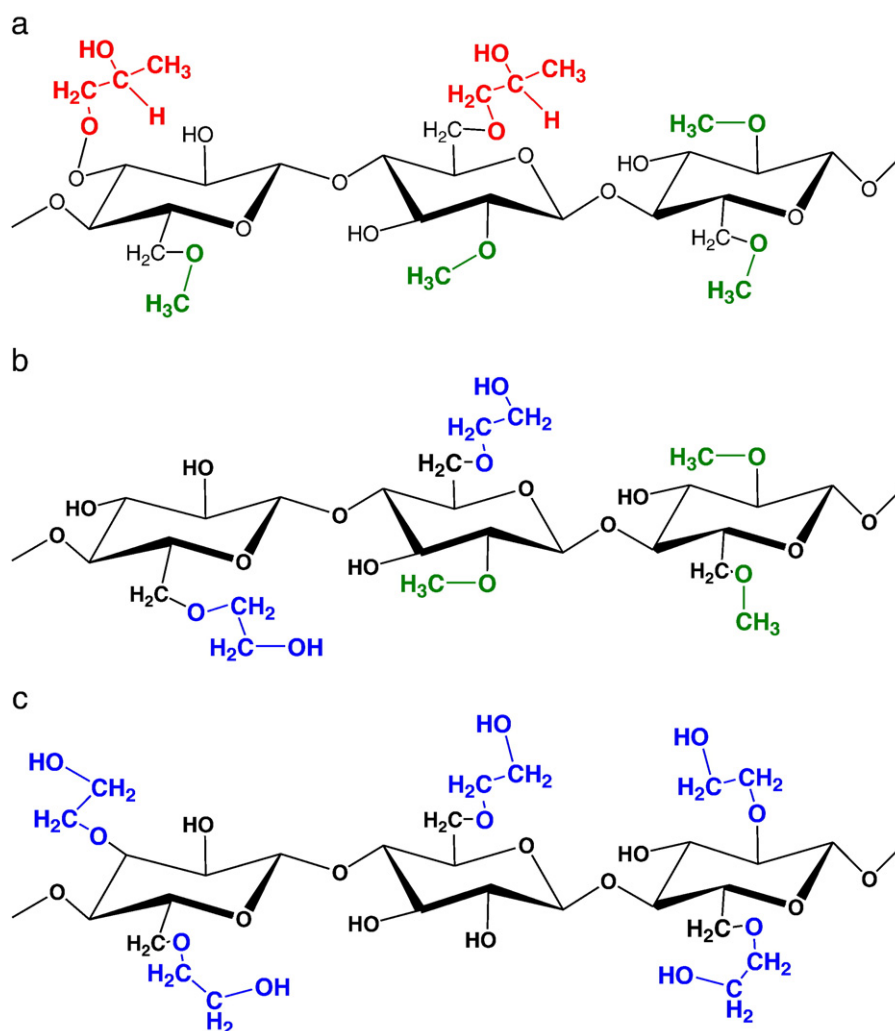E-mail address: patural@emse.fr (L. Patural).

**Fig. 1.** Structure of cellulose ethers (a: HPMC, b: HEMC, c: HEC). Substituent positions are arbitrary; they may differ slightly from one molecule to another.

vapour pressure of the admixture. Hence, as the water evaporates, the average admixture concentration increases. According to the basic thermodynamics of polymer solutions, this leads to a decrease of the water vapour pressure, due to the decrease of the water chemical potential [6]. Simultaneously, a decrease of the water mobility due to the jamming of the diffusion space by the polymer molecules is expected [7]. Both effects may be amplified by attractive polymer–water interactions. In addition, a polymer-enriched layer of low permeability (ultimately, a polymer film) may form at the mortar–air interface. As far as water loss to the substrate is concerned, the only dangerous situation is that of an unsaturated substrate. Indeed, with a fully water-saturated substrate, there is no driving force for water loss. Due to the higher osmotic pressure of the interstitial solution in the mortar, the driving force is towards pumping water from the substrate into the mortar. On the other hand, with an unsaturated substrate, a competition will set up between the capillary pressure, which drives the CE solution into the substrate, and the osmotic pressure, which drives the solvent (water) from the substrate to the mortar. In addition to the osmotic and capillary pressures, the competition is ruled by the solution and water transport properties (viscosity, diffusion coefficient).

In the present work, we choose to probe the influence of CE on the mobility of water in fresh cement pastes by Nuclear Magnetic Resonance (NMR). NMR can be used in a wide variety of modes. High resolution solid-state NMR spectroscopy has been extensively used to study the atomic structure of cement hydrates and the

measure of $T_1$ or $T_2$ relaxation times is now a classical technique to follow the microstructural evolution during hydration and setting [8]. Besides, the time evolution of the cement paste microstructure was characterized by nuclear magnetic relaxation methods at variable magnetic fields [9]. In this work, we characterized the diffusion properties of water molecules using Pulsed-Gradient Spin-Echo (PGSE) NMR on one hand and Magnetic Resonance Imaging (MRI) on the other hand. PGSE NMR is probably one of the most convenient and reliable methods to measure diffusion coefficient [10,11]. It is non-invasive, it does not involve the introduction of a chemical tracer and the system is kept at equilibrium. Moreover, in anisotropic materials, the self-diffusion tensor can be extracted from a set of measurements performed along well-chosen non-collinear directions [12,13]. PGSE NMR has been widely applied to a variety of porous materials [14]. In cement-based materials, it has been used to monitor moisture and salt transport inside concrete [15] and water absorption in mortars [16].

In the second part of the paper, MRI was used to follow water diffusion in cement pastes at large length scale (a few millimeters). In comparison with PGSE NMR which gives dynamical information at pore scale (~10 μm), the MRI length scale is about 1000× larger. MRI is extensively used as a medical diagnostic tool but it is also recognized as an important tool for non medical applications, especially in materials research and process engineering [10]. Many of these applications depict a fluid, usually water, in porous inorganic materials and highlight the dynamics of the internal water distribution during

capillary flow [17]. Generally speaking, MRI is a suitable technique to follow the diffusion of a solvent in complex structures. For instance, in order to study water diffusion in colloidal gels by $^1H$ MRI, Duval et al. followed the time-dependence of the one-dimensional proton ($^1H$) profiles during water interdiffusion between a pieces of $H_2O$-based Laponite gel and a piece $D_2O$-based gels in close contact [18]. In spite of the complex structure and the high modulus of this kind of gel, the water self-diffusion coefficient was only marginally smaller than that of bulk water.

Our investigation of the water retention mechanism and water mobility in CE-admixed mortars is organized as follows. First, water retention was measured for all CE-admixed mortars using standard methods of the mortar industry. Then, the effect of the CE on the self-diffusion coefficient of water in polymer solution was assessed using PGSE NMR. Afterwards, the water diffusion between admixed cement pastes and a substrate was studied. Finally, interdiffusion imaging experiments between $H_2O$-based and $D_2O$-based cement pastes were performed. As will be demonstrated, very little influence of the CE on the water mobility in these various situations was detected, in spite of their strong water retention properties.

## 2. Materials and experimental methods

### 2.1. Mineral and organic products

Cement pastes were prepared with white cement in order to minimize the $Fe^{3+}$ amount due to $C_4AF$ in the material. Indeed, ferromagnetic and paramagnetic constituents enhance the NMR relaxation kinetics, thus leading to very poor signals during NMR measurements. Chemical analysis of this cement was performed by X-ray fluorescence spectroscopy (XRF). The phase compositions were calculated using Bogue's formula with a correction on CaO due to sulfates [19]. The cement composition is given in Table 1. Each analysis was performed three times with the results averaged for the three measurements.

For NMR experiments, cement pastes were prepared with a water/cement ratio equal to 0.7 in order to have an appropriate consistency. Indeed, preliminary tests with various water/cement ratios, including the formulation imposed by the CEReM (W/C = 1, Section 2.2) [20], provided inadequate consistencies. With such high water to cement ratio, bleeding problems appeared.

The admixture amount was equal to 0.27% (regarding cement). The characteristics of the eight cellulose ethers selected for the study are summarized in Table 2. The number of substituted hydroxyl groups per anhydroglucose unit is expressed as degree of substitution (DS). Moreover the molar ratio of alkoxy groups in the side chains to cellulose is expressed as the average molecular substitution (MS) [21]. The cellulose ether weight-average molecular mass ($\overline{M}_W$) was determined using size exclusion chromatography [22].

In the MRI experiments, plaster of Paris ($CaSO_4$, ½ $H_2O$) was used as a substrate. It was characterized by mercury intrusion porosimetry. The total porosity of this material was 64.7% and the average pore size diameter was approximately 545 nm.

### 2.2. Water retention

For the water retention measurements, mortars were prepared according to the CEReM mixture proportions: 65% sand, 30% cement, 5% filler with a water/cement ratio equal to 1 [20]. Mixing procedure was in accordance with EN 196-1 [23]. Admixture amount (0.27%)

**Table 1**
Phase composition of the white cement.

| Phases | $C_3S$ | $C_2S$ | $C_3A$ | $C_4AF$ | Sulfates |
|---|---|---|---|---|---|
| Phase composition (%) | 68.8 ± 0.3 | 10.4 ± 0.7 | 10.5 ± 0.1 | 1.0 ± 0.1 | 7.5 ± 0.1 |

**Table 2**
Cellulose ethers panel.

| HEMC | $\overline{M}_w$ (kDa) | Hydroxyethyl group (% $OC_2H_4OH$) | MS | Methoxy group (% $OCH_3$) | DS |
|---|---|---|---|---|---|
| C2 | 180 | 4.8 | 0.15 | 27.4 | 1.7 |
| C4 | 380 | 4.8 | 0.15 | 27.4 | 1.7 |
| C6 | 630 | 4.4 | 0.14 | 28.3 | 1.8 |
| **HPMC** | $\overline{M}_w$ (kDa) | Hydroxypropyl group (% $OC_3H_6OH$) | MS | Methoxy group (% $OCH_3$) | DS |
| J1 | 225 | 2.98 | 0.1 | 28.2 | 1.8 |
| J2 | 630 | 2.98 | 0.1 | 28.2 | 1.8 |
| **HEC** | $\overline{M}_w$ (kDa) | Hydroxyethyl group (% $OC_2H_4OH$) | MS | | |
| H1 | 45 | 45.3 | 1.9 | | |
| H4 | 430 | 51.2 | 2.3 | | |
| H7 | 790 | 52.5 | 2.4 | | |

was in addition to the total dry mixture (i.e. cement, sand and filler). In consequence, the CE concentration, for this formulation was 9 g $L^{-1}$. Siliceous sand (ref. DU 0.1/0.35) was used, in agreement with NF EN 13139 standard [24]. The filler was calcium carbonate ($CaCO_3$). Grey Portland cement CEM I 52.5 R was used, according to EN 197-1 [25].

The water retention capacity can be assessed using diverse testing methods. One of these methods used is described in the DIN 18 555-7 standard [26]. With this method, a freshly-mixed mortar is in contact with filter paper, thereby simulating the action of an absorptive substrate.

DIN measurements have to be performed 5 min after mixing. The water retention capacity of a freshly-mixed mortar is characterized by the mass of water it retains after capillarity action of an absorbent substrate. The standardised apparatus is described in Fig. 2.

The mortar (3) was poured into the ring. Then, knowing that the water content of the tested mortar was equal to 23%, for CEReM formulation, the water retention was calculated by weight differences (Eq. (1)).

$$WR = 100 - \frac{m_{fp}}{m_m} \times 100 \tag{1}$$

Where $m_{fp}$ is the quantity of water retained by the filter paper and $m_m$ is the quantity inside the studied mortar.

### 2.3. NMR equipment

All proton NMR measurements were performed using a Bruker DSX100 spectrometer operating at a proton ($^1H$) frequency of 100 MHz with a 2.35 T superconducting magnet. A microimaging probehead (Micro5 Bruker) with gradient coils in three perpendicular directions was used to generate magnetic field gradients along any arbitrary directions. All experiments were performed at room
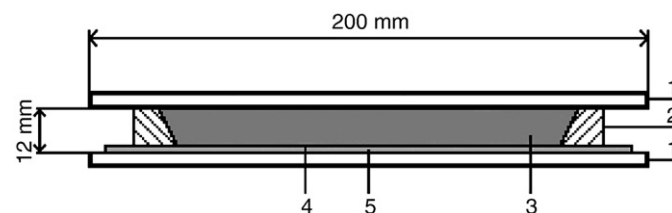


**Fig. 2.** DIN 18 555-7 test arrangement for determining the water retention of freshly mixed mortars (1: two plastic plates, 2: a conical plastic ring, 3: mortar, 4: filter paper [190×190 mm], 5: a nonwoven tissue).

temperature (293 K). All samples were introduced into a 10 mm-diameter standard NMR tube, with an inner diameter of about 8.5 mm.

## 2.4. Longitudinal relaxation time ($T_1$) measurements

The longitudinal relaxation time $T_1$ is the characteristic time for re-establishing thermal equilibrium of the longitudinal component of the magnetization vector [27]. In other words, the $T_1$ value corresponds to the time required for the magnetization to recover 63% of its initial value after being flipped into the magnetic transverse plane by a 90° Radio Frequency pulse. To ensure that the magnetization relaxes to its thermal equilibrium before each pulses sequence, the repetition time was chosen up to 5 $T_1$, i.e. 15 s (corresponding to a recovery of about 99.3% of the equilibrium state). The longitudinal relaxation times were measured in all samples using the standard inversion-recovery pulse sequence (180°–$\tau$ 90–Acq.) [28], with a pulse width of the 90° pulse equal to 7.75 µs and a delay $\tau$ varying between 250 ms and 15 s (8 steps). The $T_1$ values were then obtained by fitting the maximum amplitude of the NMR spectra versus the delay $\tau$ by the following recovery equation (Eq. (2)):

$$M_z = M_0 \left[ 1 - 2 \times \exp\left( -\frac{\tau}{T_1} \right) \right] \qquad (2)$$

## 2.5. Self-diffusion PGSE measurements

Water self-diffusion coefficient measurements in CE solutions were performed by using the PGSE NMR method originally described by Stejkal and Tanner [11]. In this pulse sequence, depicted in Fig. 3, the proton $^1$H spins are labelled at time $t=0$ with respect to their positions in a given direction ($O_i$) by applying a 90°-pulse of magnetic field gradient along this direction. After an evolution time $\Delta$ called diffusion time, a second 180°-pulse of magnetic field gradient is then applied. This second gradient pulse cancels the effect of the first one, unless the spins have moved during the time $\Delta$ along the same direction ($O_i$). If the spins have diffused along this chosen direction ($O_i$), the second gradient pulse does not refocus the entire spins signal and the echo intensity is less intense. So, this decrease of the echo amplitude is a function of the self-diffusion coefficient $D$, and the echo attenuation $E(q,\Delta)$ measured using this method is given by the following equation:

$$E(\Delta, \Delta) = \frac{I(q,\Delta)}{I(0,\Delta)} = \exp\left[ -4\pi^2 q^2 D(\Delta - \delta/3) \right] \qquad (3)$$
$$= \exp\left[ -\gamma^2 g^2 \delta^2 D(\Delta - \delta/3) \right]$$

where $q = \frac{\gamma g \delta}{2\pi}$, with $\gamma$ the gyromagnetic ratio of the proton ($\gamma = 2.675 \times 10^8$ rad s$^{-1}$ T$^{-1}$), $g$ is the intensity of the pulsed magnetic field gradient, $\delta$ its duration, $\Delta$ the diffusion time and $D$ the self-diffusion coefficient, $I(q,\Delta)$ and $I(0,\Delta)$ being the echo intensities measured with and without the magnetic field gradient $g$, respectively. This method, based on the $T_2$ spin-echo sequence [29], is limited by the value of the transverse relaxation time $T_2$ that dictates the maximal value of the diffusion time $\Delta$ and the magnetic field gradient duration $\delta$. In our experiments, pulse sequence parameters were fixed at 20 ms for $\Delta$ and 1 ms for $\delta$, whereas $g$ was varied from 0 to 1.5 T m$^{-1}$ (8 steps). By performing a series of experiments with variable gradient intensities $g$, from the slope of the echo attenuation $\ln[E(q,\Delta)]$ versus the quantity $-\gamma^2 g^2 \delta^2 (\Delta - \delta/3)$, the self-diffusion coefficient $D$ is calculated.

## 2.6. Imaging experiments at the paste/unsaturated substrate interface

A standard one-dimensional spin-echo sequence [10] was used to obtain 1D profiles with a repetition time (TR) of 1 s. Depending on the length of the sample, the field of view was taken varying between 20 mm and 25 mm leading to a spatial resolution of 39 µm and 49 µm with 512 pixels along the profile. From these 1D profiles, the water concentration can be determined inside the sample at a given time. To quantify the diffusion process, the migration of the water inside the different experiment configurations is detected by the analysis of a set of 1D profiles acquired at constant time intervals.

The experimental procedure was the following: the fresh cement paste was introduced into the tube 15 min after mixing. Then, as soon as possible, a piece of hardened plaster of Paris was put into contact with the paste, as illustrated on Fig. 4. The one-dimensional proton concentration profiles along the tube axis were then acquired according to a constant temporal interval (a few minutes typically).

Several substrates were tested. Plaster of Paris was chosen as the most convenient substrate. Indeed, its affinity as regards to water and appropriate porosity lead to relatively short-time analysis.

## 2.7. Interdiffusion imaging experiments at the paste/paste interface

In the last series of experiments, the influence of CE on water mobility was measured at the interface between two fresh cement pastes. These experiments were performed using two open pieces of glass tubes filled with fresh cement paste. They were then assembled in a larger NMR glass tube as displayed in Fig. 5. One was prepared with water and the other with heavy water. The one-dimensional proton concentration profile along the cylinder axis was then followed as a function of time. Fig. 5 shows the three studied configurations. In spite of the cement hydration delay in presence of D$_2$O [30,31], experiments were not affected because they were
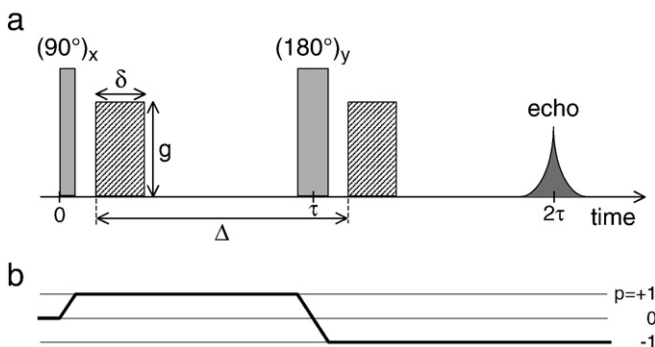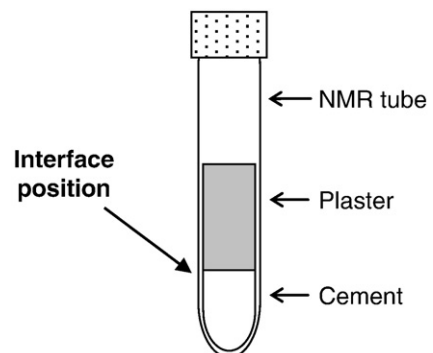


**Fig. 3.** (a) Schematic view of the Pulsed-Gradient Spin-Echo (PGSE) sequence used for the measurement of the self-diffusion coefficients. (b) Coherence transfer pathway ($p = 0 \rightarrow +1 \rightarrow -1$) resulting from an adequate phase cycling.



**Fig. 4.** Sample configuration for the study of water diffusion at the interface between a fresh cement paste and a piece of hard plaster of Paris.
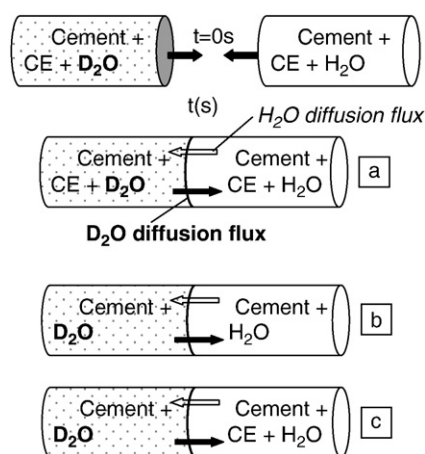
**Fig. 5.** Inter-diffusion imaging experiments at the interface between two fresh pastes (a: admixed cement pastes; b: non-admixed cement pastes; c: only one side contains CE).

performed during the dormant period. Besides, the results can be relatively compared because the conditions were the same for the three configurations and absolute values were not determined.

The cellulose ether HPMC J2 (see Table 2) was chosen for this experiment, due to its strong water retention capacity to enhance the observed phenomenon.

## 3. Results

### 3.1. Water retention of freshly-mixed mortars

The water retention capacity of each admixed mortar was assessed using the standard DIN method. The results are presented in Table 3. The cellulose ethers improved water retention up to 92.3% for HEC H1, to 99.5% for HPMC C6. With respect to the water retention capacity of the non-admixed mortar (60.2%), this represents a very large increase. These figures are qualitatively in agreement with the results of Pourchez et al. [4] obtained with other HPMC and HEMC admixtures.

### 3.2. Relaxation and water proton self-diffusion in CE solution

The first step of our investigation is to know whether the cellulose derivatives affect the $T_1$ longitudinal relaxation time and/or the proton self-diffusion coefficient $D$ in an aqueous solution (prepared with distilled water). For this purpose, both parameters were measured in CE solutions for two CE solutions: HEC H1 and HEMC C4. These polymers were chosen because they provide to the mortar critical values of water retention (Section 3.1). Experiments were performed with two H1 concentrations: $1\,g\,L^{-1}$ and $9\,g\,L^{-1}$, respectively, to reach the CEReM mortar concentration. The results for HEC are shown in Table 4. The self-diffusion coefficient of water ranged from $2.02 \times 10^{-9}\,m^2\,s^{-1}$ in distilled water to $1.98 \times 10^{-9}\,m^2\,s^{-1}$ in the most concentrated H1 solution. Considering the fluctuations

**Table 3**
DIN water retention results (Section 3.1) and MRI steady state times, Ts (Section 3.3).

| Cellulose ether | | WR_DIN (%) | Ts (min) |
|---|---|---|---|
| Control | – | (60.2 ± 0.2) | (4 ± 1) |
| HEC | H1 | (92.3 ± 0.6) | (28 ± 2) |
| | H4 | (98.2 ± 0.4) | (130 ± 2) |
| | H7 | (98.6 ± 0.4) | (106 ± 2) |
| HEMC | C2 | (94.2 ± 0.6) | (92 ± 3) |
| | C4 | (99.3 ± 0.5) | (162 ± 3) |
| | C6 | (99.5 ± 0.2) | (185 ± 3) |
| HPMC | J1 | (96.4 ± 0.1) | (132 ± 3) |
| | J2 | (99.4 ± 0.1) | (178 ± 3) |

**Table 4**
PGSE NMR self-diffusion coefficient of water in cellulose ether H1 solutions.

| | Relaxation time $T_1$ (s) | Relaxation rate $R_1 = 1/T_1$ (s$^{-1}$) | Self-diffusion coefficient $D$ ($10^{-9}$ m²s$^{-1}$) |
|---|---|---|---|
| Distilled water | 2.77 | 0.361 | 2.02 |
| H1 solution, [H1] = 1 g L$^{-1}$ | 2.78 | 0.360 | 2.05 |
| H1 solution, [H1] = 9 g L$^{-1}$ | 2.74 | 0.365 | 1.98 |

($D = 2.05 \times 10^{-9}\,m^2\,s^{-1}$ at $1\,g\,L^{-1}$), this cannot be considered as a significant decrease. The conclusion is that HEC H1 does not significantly modify the proton or water self-diffusion coefficient from the polymer solutions with concentrations ranging from 1 to $9\,g\,L^{-1}$.

After the results were obtained, a larger CE concentration range, up to $60\,g\,L^{-1}$, was investigated with HEMC C4. The results are shown in Fig. 6.

In the concentration range from 10 to $60\,g\,L^{-1}$, the proton self-diffusion coefficient decreased from $1.96 \times 10^{-9}\,m^2\,s^{-1}$ to $1.81 \times 10^{-9}\,m^2\,s^{-1}$. This represents a mere 10% reduction with respect to pure water. At $9\,g\,L^{-1}$, which is the CE concentration in the reference CEReM mortar, the decrease of $D$ amounts to about 2%. In relative terms, this is vastly weaker than the increase of water retention measured on mortars at the same CE concentration (Section 3.1).

In conclusion, at the concentrations used in mortars formulation, CE does not significantly modify the water self-diffusion coefficient in aqueous solutions.

### 3.3. Water mobility at the cement paste/substrate interface

Using MRI, one-dimensional proton concentration profiles between a fresh cement paste and a piece of (initially) dry plaster were recorded. Fig. 7a and b displays the signal intensity profiles along the z-axis for a neat cement paste and a cement paste admixed with H1, respectively. The left parts of the curves represent the cement paste and the right ones are the porous substrate. Capillary invasion of the substrate starts as soon as contact is established. Note that $t = 0$, in Fig. 7, corresponds to the time when the first profile record was
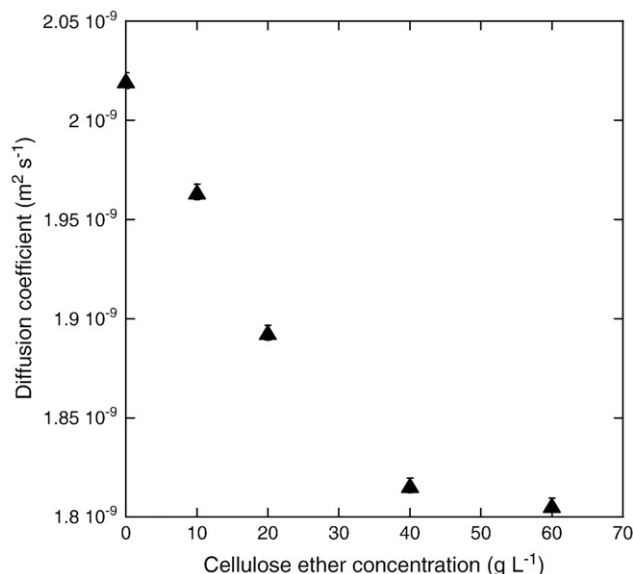


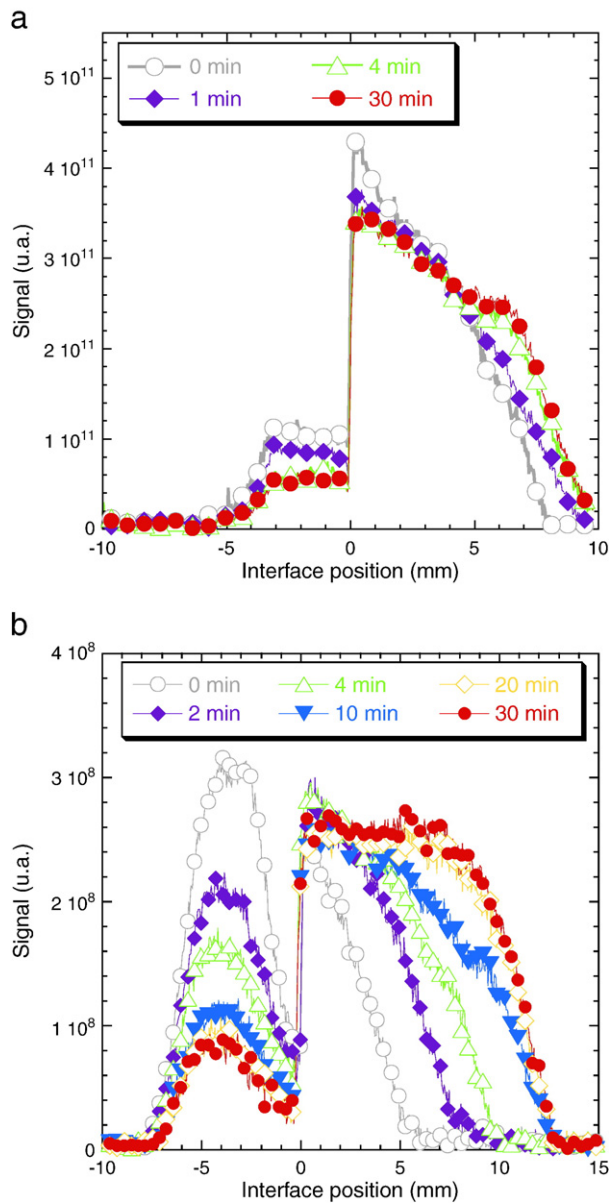**Fig. 6.** Influence of the HEMC C4 concentration on the water self-diffusion coefficient in polymer solutions.

**Fig. 7.** One-dimensional proton concentration profiles: a: cement paste/plaster; b: cement paste admixed with HEC H1/plaster.



**Fig. 8.** a. Integration of one-dimensional proton concentration profile (cement paste/ plaster). b. Integration of one-dimensional proton concentration profile (cement paste + H1/ plaster).

completed, which was approximately 1 min after contact. This explains that at $t=0$ significant suction of water by the substrate was already observed. For admixed cement paste, in approximately 30 min, the substrate was homogeneously saturated.

A series of profiles were recorded for each cellulose derivative. To estimate the CE effect on the suction process, the profiles were integrated in order to determine when a steady state was achieved for the system. Then, the curves were normalized to 1. As illustrated in Fig. 8a and b, the normalized integral value is increasing rapidly, reaching a plateau value after a few minutes for the neat cement and about 30 min for the admixed cement. The time needed to reach 99% of the final value will be noted $Ts$. Note that the increase of the profile integral does not mean that the overall quantity of water in the paste/substrate system is increasing. The evolution stems from the fact that the relaxation times of protons are different in the paste and the substrate. In other words, the one-dimensional proton concentration profiles are weighted by the transverse relaxation times $T_2$ of protons for each part of the sample. This leads to a different sensitivity in each medium and the profile intensities cannot be directly compared each other. For non admixed cement paste,
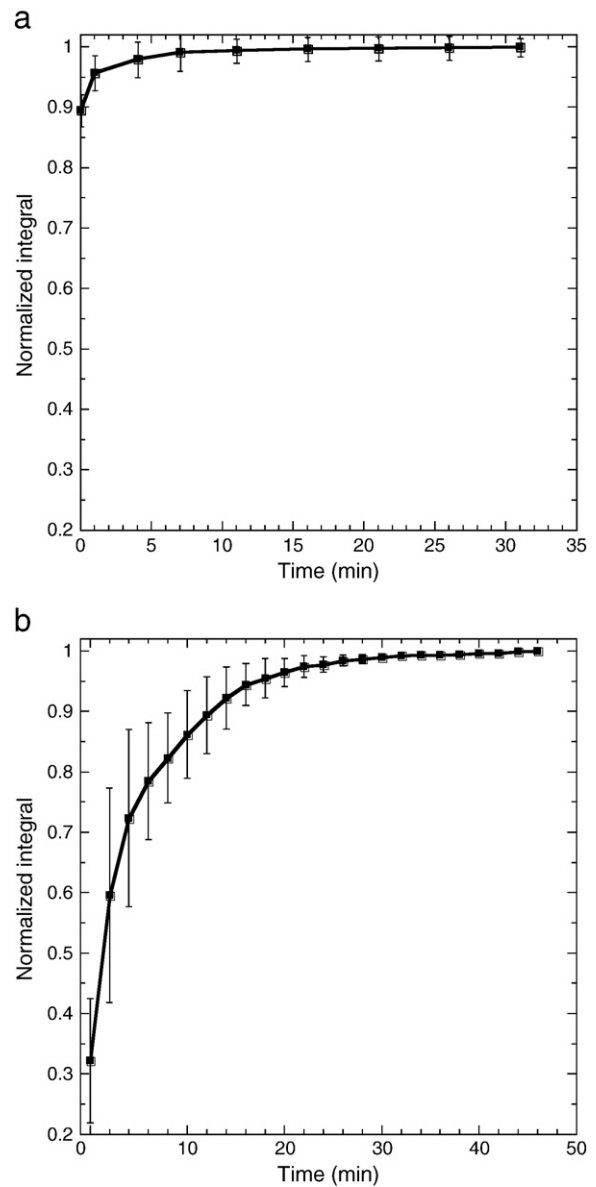
$Ts$ is equal to 4 min whereas for HEC H1, $Ts$ is equal to 28 min. The values for the other CE are tabulated in Table 3.

$Ts$ characterizes the water retention capacity of the paste in contact with a porous substrate. Therefore, a strong correlation is expected with the water retention capacity determined by the standard DIN method (Section 3.1). In the later, the amount of water absorbed by a filter paper in contact with the mortar is measured after 5 min. Indeed, when the mortar water retention capacity is plotted versus the MRI $Ts$ value, a good linear correlation is obtained (Fig. 9; $R^2=0.98$). This validates the standard DIN method and the use of filter paper as a valuable method to evaluate water retention in real mortar/substrate configurations.

### 3.4. Interdiffusion at the paste/paste interface

As explained in Section 2, three types of $H_2O/D_2O$ interdiffusion experiments at the paste/paste interface were performed. They all have in common to have $H_2O$ on one side and $D_2O$ on the other. In type (a) experiments, both sides contain CE at the same concentration. In
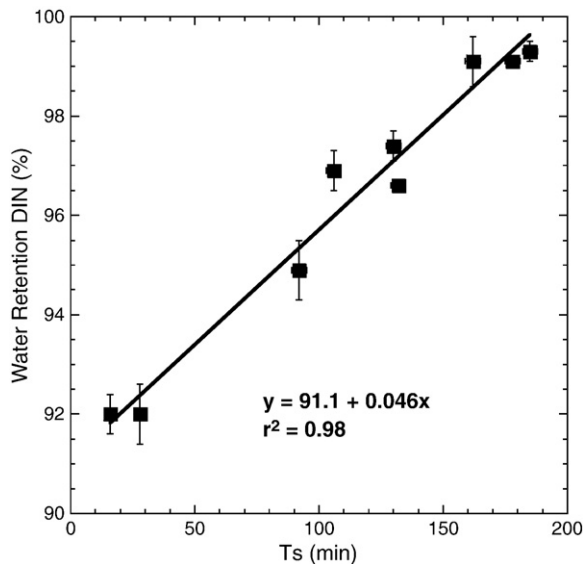
**Fig. 9.** Relationship between standard water retention measurements and MRI results.



**Fig. 10.** One-dimensional proton concentration profiles during interdiffusion at the paste/paste interface (a: $t = 0$ min; b: $t = 75$ min).

type (b), both sides are CE-free. In type (c), the $H_2O$ side contains CE whereas the $D_2O$ side does not. Fig. 10a illustrates the signal intensity profiles along the z-axis at initial time. The signal perturbations of the profiles present at the different interfaces of the sample are due to the presence of little drops of liquid (interface and top of the sample) which are generated when the two parts of the sample are put into contact. These drops of liquid also induce inhomogeneities of the magnetic susceptibility at these boundaries. These intensity profiles were normalized in order to be able to compare them to each other at later time. However, the proton amount cannot be determined using these profiles. Indeed, as already pointed out in Section 3.3, the intensity profiles do not reflect the actual proton density. They are related only to the proton density weighted by the transverse relaxation time $T_2$. Nevertheless, at initial time, for each type of experiment, the profiles were the same when both compartments were put into contact. As time went on, water molecules diffused from one side to the other. Remarkably, whatever the type of experiment and the time (25 min and 75 min), the profiles in the three types of experiments remained identical to each other (Fig. 10). Thus, water diffusion at the paste/paste interface is not affected by the presence of CE. This conclusion is valid when the CE is introduced on both sides and when it is introduced on one side only.

## 4. Discussion and conclusions

The standard DIN 18 555-7 method is used by the mortar industry to estimate the water retention capacity of admixed mortars, based on the water loss at the mortar/filter paper interface (Section 3.1). A first conclusion which can be safely drawn from the experiments reported in this paper is that, this method is reliably related to the actual water migration process occurring through the interface between a fresh cement paste and a dry porous substrate (Section 3.3). To our best knowledge, this is the first time that such a direct validation is made.

A second important conclusion related to the water retention mechanism is that, at the concentrations used in practice and even beyond, CE does not significantly modify the water self-diffusion coefficient. This was established in CE solutions (Section 3.2) and in admixed cement pastes (Section 3.4, comparison of type a with type b experiments). This is in agreement with previous studies on dilute or semi-dilute polymer and colloidal solutions or even gels [7,18]. In spite of their potentially very high viscosity and yield stress, these media are actually very "open" systems, with large and well connected solvent-
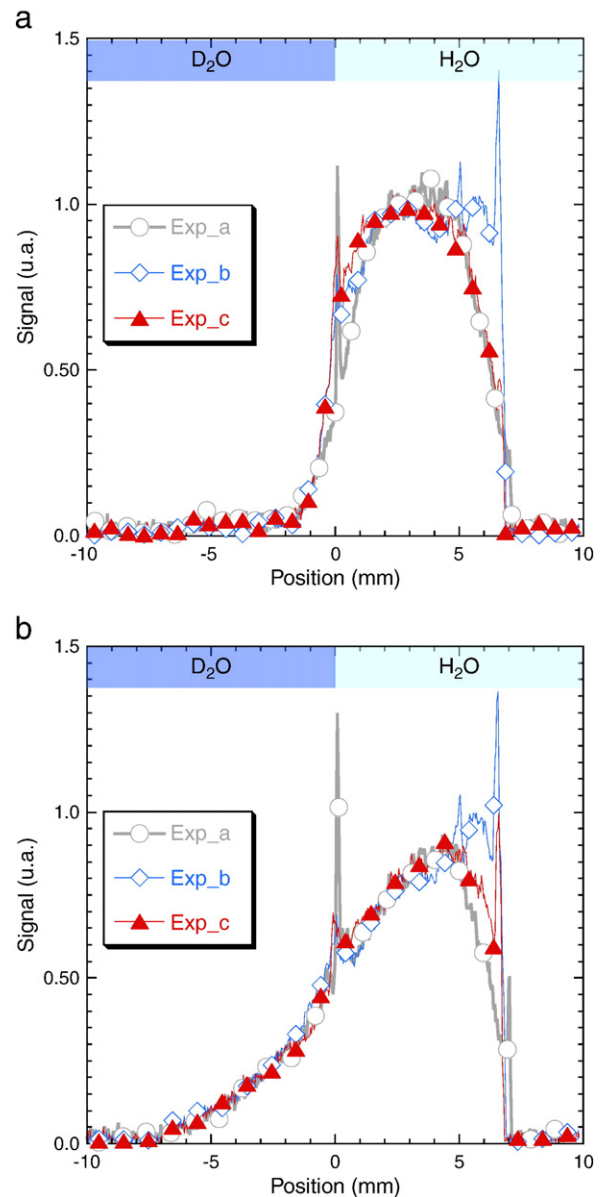
filled voids within and between the polymer molecules coils, or between the colloidal particles.

More surprising is the observation that water self-diffusion is not modified even when an osmotic gradient is counteracting the diffusion flux. This is shown by the results of type c experiments (with osmotic gradient) in Section 3.4, undistinguishable from those of type b experiments (without osmotic gradient). Of course, this does not mean that osmotic effects would remain negligible at higher CE concentrations.

What type c experiments do show (or, confirm) also is that CE do not introduce any water retention property when the admixed cement paste is applied on a water saturated substrate. Indeed, the $D_2O$-saturated admixture-free cement paste in these experiments is nothing else than a saturated substrate.

When taken together, our experiments and results lead to the conclusion that the only configuration where water mobility is strongly modified by small amounts of CE is that of a mortar/unsaturated substrate interface. This is a configuration where water loss is driven by capillary suction, not by diffusion. The flow induced

by capillary suction is itself controlled by the substrate pore pressure, which depends on pore size and interface tension *via* Laplace's equation, and by the fluid viscosity [32]. This suggests that the rheological properties of the aqueous CE solutions may be the key properties for water retention. However, this working hypothesis is against the common acceptance that other viscosity enhancing admixtures such as high molecular weight PEO (polyethylene oxides) and starches are less effective than CE. Alternatively, one may consider the formation of a thin CE- and fine particles-enriched filter cake at the mortar/substrate interface, similarly to what happens at the fluid/rock interface with polysaccharide-based drilling muds in oil well drilling [33]. In any case, further work is necessary to solve the question. The main point established in this work is that an organic admixture may be a strong water retaining agent without modifying the mobility of water in either in solution or paste.

## Acknowledgements

## References

[1] S. Mansoutre, P. Colombet, H. Van Damme, Water retention and granular rheological behavior of fresh $C_3S$ paste as a function of concentration, Cem. Concr. Res. 29 (1999) 1441–1453.

[2] A. Peschard (2003). Aspects physico-chimiques de l'interaction ciment-poly-saccharides. PhD thesis. Ecole Nationale Supérieure des Mines de Saint-Etienne.

[3] J. Pourchez (2006). Aspects physico-chimiques de l'interaction des éthers de cellulose avec la matrice cimentaire. PhD thesis. Ecole Nationale Supérieure des Mines de Saint-Etienne.

[4] J. Pourchez, A. Peschard, P. Grosseau, R. Guyonnet, B. Guilhot, F. Vallée, HPMC and HEMC influence on cement hydration, Cem. Concr. Res. 36 (2006) 288–294.

[5] J. Pourchez, B. Ruot, J. Debayle, E. Pourchez, P. Grosseau, Some aspects of cellulose ethers influence on water transport and porous structure of cement-based materials, Cem. Concr. Res. 40 (2010) 242–252.

[6] H. Kuhn, D.H. Waldeck, H.-D. Försterling, Principles of Physical Chemistry, Wiley-Interscience, 2009.

[7] B. Penke, S. Kinsey, S.J. Gibbs, T.S. Moerland, B.R. Locke, Proton diffusion and T1 relaxation in polyacrylamide gels: a unified approach using volume averaging, J. Magn. Reson. 132 (1998) 240–254.

[8] P. Colombet, A.-R. Grimmer, H. Zanni, P. Sozzani, Nuclear magnetic resonance spectroscopy of cement-based materials, Springer-Verlag, Berlin and Heidelberg GmbH & Co. K, 1998.

[9] J.-P. Korb, NMR and nuclear spin relaxation of cement and concrete materials, Curr. Opin. Colloid Interface Sci. 14 (2009) 192–202.

[10] P.T. Callaghan, Principles of nuclear magnetic resonance microscopy, Clarendon Press, Oxford, 1991.

[11] E.O. Stejskal, J.E. Tanner, Spin diffusion measurements — spin echoes in presence of time-dependent field gradient, J. Chem. Phys. 42 (1965) 288–292.

[12] P. Porion, S. Rodts, M. Al-Mukhtar, A.-M. Faugère, A. Delville, Anisotropy of the solvent self-diffusion tensor as a probe of nematic ordering within dispersions of nanocomposites, Phys. Rev. Lett. 87 (2001) 208–302.

[13] P. Porion, A.-M. Faugère, A. Delville, $_1H$ and $_7Li$ NMR pulsed gradient spin echo measurements and multiscale modeling of the water and ionic mobility within aqueous dispersions of charged anisotropic nanoparticles, J. Phys. Chem. C 112 (2008) 11893–11900.

[14] V. Busignies, P. Porion, B. Leclerc, P. Evesque, P. Tchoreloff, Application of PGSTE-NMR technique to characterize the porous structure of pharmaceutical tablets, Eur. J. Pharm. Biopharm. 69 (2008) 1160–1170.

[15] G.H.A. Van Der Heijden, R.M.W. Van Bijnen, L. Pel, H.P. Huinink, Moisture transport in heated concrete, as studied by NMR, and its consequences for fire spalling, Cem. Concr. Res. 37 (2007) 894–901.

[16] L. Pel, K. Hazrati, K. Kopinga, J. Marchand, Water absorption in mortar determined by NMR, Magn. Res. Imag. 16 (1998) 525–528.

[17] R.J. Gummerson, C. Hall, W.D. Hoff, R. Hawkes, G.N. Holland, W.S. Moore, Unsaturated water flow within porous materials observed by NMR imaging, Nature 281 (1979) 56–57.

[18] F.P. Duval, P. Porion, A.M. Faugère, H. Van Damme, An NMR investigation of water self-diffusion and relaxation rates in controlled ionic strength laponite sols and gels, J. Colloid Interface Sci. 242 (2001) 319–326.

[19] H.F.W. Taylor, Cement Chemistry, 2nd editionAcademic Press Thomas Telford, 1997.

[20] B. Ruot, T. Goto, J. Pourchez, Some aspects of cellulose ethers and latexes influence on the properties of cement-based materials — examples of results obtained within the CEReM, Proceedings of the VII SBTA (7° Symposio Brasileiro De Tecnologia Das Argamassas), 2007.

[21] F. Crössmann, W. Klaus, Wasserlösliche Celluloseäther im Spiegel der Anwendungstechnik, Collection of publication of a group of authors of Kalle, branch of Hoechst AG, 1974 Wiesbaden-Biebrich.

[22] C. Clasen, W.M. Kulicke, Determination of viscoelastic and rheo-optical material functions of water-soluble cellulose derivatives, Prog. Polym. Sci. 26 (2001) 1839–1919.

[23] EN 196-1, Methods of testing cement — Part 1: determination of strength, 2006.

[24] NF EN 13139, Granulats pour mortiers — Spécifications des caractéristiques des granulats et fillers utilisés dans les mortiers, 2003.

[25] EN 197-1, *Cement. Part 1: Composition, specification and conformity criteria for common cements*, 2001.

[26] Standard DIN 18555-7, *Testing of mortars containing mineral binders; part 7: determination of water retentivity of freshly mixed mortar by the filter plate method*, Deutsches Institut für Normung, 2000.

[27] A. Abragam, The principles of nuclear magnetism, Clarendon Press, Oxford, 1961.

[28] M.L. Martin, J.J. Delpuech, G.J. Martin, Practical NMR spectroscopy, Heyden, London, 1980.

[29] E.L. Hahn, Spin echoes, Phys. Rev. 80 (1950) 580–594.

[30] T.C. King, C.M. Dobson, S.A. Rodger, Hydration of tricalcium silicate with $D_2O$, J. Mater. Sci. Lett. 7 (1988) 861–863.

[31] J.J. Thomas, H.M. Jennings, A.J. Allen, The surface area of cement paste as measured by neutron scattering: evidence for two C-S-H morphologies, Cem. Concr. Res. 28 (1998) 897–905.

[32] Y. Guéguen, V. Palciauskas, Introduction to the physics of rocks, Princeton University Press, 1994.

[33] E.B. Nelson, D. Guillot, Well cementing, Schlumberger, 1990.